Atmospheric rivers moisture sources from a Lagrangian perspective

A. M. Ramos[1], R. Nieto[2], R. Tomé[1], L. Gimeno[2], R.M. Trigo[1], M.L.R Liberato[1,3], D. A. Lavers[4]

[1] {Instituto Dom Luiz, Faculdade de Ciências, Universidade de Lisboa, Lisbon, Portugal}

[2] {EPhysLab (Environmental Physics Laboratory), Facultade de Ciencias, Universidade de Vigo, Ourense, Spain}

[3] {Escola de Ciências e Tecnologia, Universidade de Trás-os-Montes e Alto Douro, Vila Real, Portugal}

[4] {Center for Western Weather and Water Extremes, Scripps Institution of Oceanography, University of California, San Diego, La Jolla, California, United States}

Correspondence to: A. M. Ramos (amramos@fc.ul.pt)

Abstract

An automated atmospheric river (AR) detection algorithm is used for the North Atlantic Ocean Basin, allowing the identification of the major ARs affecting Western European coasts between 1979 and 2012 over the winter half-year (October to March). The entire western coast of Europe was divided into five domains, namely the Iberian Peninsula (9.75ºW; 36ºN – 43.75ºN), France (4.5ºW; 43.75ºN – 50ºN), UK (4.5ºW; 50ºN-59ºN), Southern Scandinavia and the Netherlands (5.25ºE; 50ºN-59ºN), and Northern Scandinavia (5.25ºE; 59ºN – 70ºN). Following the identification of the main ARs that made landfall in Western Europe, a Lagrangian analysis was then applied in order to identify the main areas where the moisture uptake was anomalous and contributed to the ARs reaching each domain. The Lagrangian dataset used was obtained from the FLEXPART model global simulation from 1979 to 2012 and was forced by ERA-Interim reanalysis on a 1º latitude-longitude grid.

The results show that, in general, for all regions considered, the major climatological areas for the anomalous moisture uptake extend along the subtropical North Atlantic, from the Florida Peninsula (northward of 20ºN) to each sink region, with the nearest coast to each sink region always appearing as a local maximum. In addition, during AR events the Atlantic subtropical source is reinforced and displaced, with a slight northward movement of the sources found when the sink region is positioned at higher latitudes. In conclusion, the results confirm the anomalous advection of moisture linked to ARs from subtropical ocean areas, but also the existence of a tropical source, together with mid-latitude anomaly sources at some locations closer to AR landfalls.

1 Introduction

Atmospheric Rivers (ARs) are relatively narrow (on average ~500 Km) pathways of water vapour (WV) transport that can extend for thousands of kilometres, contain large amounts of WV, and are often accompanied by strong winds (Zhu and Newell, 1998; Ralph et al., 2004). According to several authors (Ralph et al. 2004; 2005), their properties include a concentrated band of enhanced WV in the lower troposphere and a pre-cold frontal low level jet (LLJ) due to the temperature gradient across the cold front (Neiman et al., 2008; Ralph et al. 2004; Ralph et al. 2005).

The attribution of the terms ‘atmospheric river’ or ‘tropospheric river’ and their genesis caused some debate in the scientific community. Recently, some agreement has been achieved (Dettinger et al., 2015) regarding the relationships between ARs, warm conveyor belts (WCBs), and tropical moisture exports (TMEs). The term WCB refers to the zone of dynamically uplifted heat and vapour transport close to a mid-latitude cyclone. This vapour is often transported to the WCB by an AR, and the result of the uplift is heavy rainfall that generally marks the downwind end of an AR, provided that the AR has not experienced orographic uplift (upslope flow), accompanied by rainout over mountains earlier on its approach to the WCB. TMEs are zones of intense vapour transport out of the tropics, vapour that is frequently conducted by ARs towards cyclones and WCBs. TMEs can provide important vapour sources for ARs, but most ARs also incorporate mid-latitude sources and convergences of vapour along their paths (Dettinger et al., 2015; Sodemann and Stohl, 2013). In addition, the role of ARs in explosive cyclogenesis over the North Atlantic Ocean has been shown for three extra-tropical cyclones (Klaus; Gong and Stephanie), all of which had major socio-economic impacts in parts of Europe (Ferreira et al., 2016).

The importance of ARs in extreme precipitation events and floods has been analysed in detail for the west coast of the USA (particularly for California) over the last decade (e.g., Dettinger et al., 2011; Neiman et al., 2008; Ralph et al., 2004; Ralph et al., 2013).

For Europe, Lavers and Villarini (2013) showed that ARs are responsible for many annual maximum precipitation days in Western Europe, with the relationship being stronger along the western European seaboard, and with some areas having up to eight of their top 10 annual maxima related to ARs. It was also shown that 40-80% of winter floods in the UK are associated with persistent ARs and that that these ARs are critical in explaining the 10 largest winter flood events in a range of British rivers basins since 1970 (Lavers et al., 2011; Lavers et al., 2012). For the Iberian Peninsula, Ramos et al. (2015) showed that ARs play an overwhelming role in most extreme precipitation days, decreasing in importance for less extreme precipitation days. Moreover, over the North Atlantic Ocean and for the island of Madeira, in particular, the association between extreme precipitation and ARs was also established (Couto et al., 2012; Couto et al., 2015).

In addition, the importance of ARs in a few particular cases of extreme precipitation in Europe has also been analysed in some detail. Liberato et al. (2012) discussed an extreme precipitation event associated with an AR occurring in the city of Lisbon, Portugal, in November 1983, which produced flash flooding, urban inundations, and landslides causing considerable damage to infrastructure and human fatalities. On the Norwegian southwest coast, an extreme precipitation event occurred in September 2005 and was also shown to be directly linked with an AR (Stohl et al., 2008). More recently, Trigo et al. (2014) considered the record precipitation and flood event in the Iberia Peninsula of December 1876 and highlighted the importance of ARs in this historical event.

The association between ARs and modes of low frequency variability has already been addressed, with the Scandinavian pattern having a negative correlation with the occurrence of ARs in Britain (Lavers et al., 2012), while it is the North Atlantic Oscillation that controls their occurrence to a certain extent in the rest of Europe (Lavers and Villarini, 2013). In addition, Ramos et al. (2015) showed that for the particular case of the Iberian Peninsula, the East Atlantic pattern also plays a major role in explaining the annual variability of ARs.

The increasing attention to the topic of ARs is confirmed by the publication of two recent reviews, with Ralph and Dettinger (2011) emphasising the multiple studies of ARs striking the western coast of the USA, while Gimeno et al. (2014) focused on the structure, methods of detection, impacts, and dynamics of ARs.

Bao et al. (2006) suggested that the moisture present in ARs has two main origins, namely local moisture convergence along the front of extra-tropical cyclones, and direct poleward transport of tropical moisture, suggesting that they play an important role in the water cycle, especially in transporting moisture from the tropics to the mid and high latitudes. In this context Dacre et al. (2015) analysed selected cases of the transport of water vapour within a climatology of wintertime North Atlantic extra-tropical cyclone. In this particular study, the possibility was discussed that ARs are formed by the cold front that sweeps up water vapour in the warm sector as it catches up with the warm front. This causes a narrow band of high water vapour content to form ahead of the cold front at the base of the warm conveyor belt airflow. Thus, according to Dacre et al. (2015), water vapour in the warm sector of the cyclone, rather than long-distance transport of water vapour from the subtropics, is responsible for the generation of ARs. According to Dettinger et al. (2015) it seems that a combination of the two points of view are valid because TMEs can provide important vapour sources for ARs, but most ARs also incorporate mid-latitude sources and convergences of vapour along their paths.

To the best of our knowledge studies dealing with moisture sources from a Lagrangian point of view along the paths of ARs are scarce and have only been developed for selected case studies. For instance, Moore et al. (2012) used Lagrangian trajectories associated with heavy flooding rainfall in Nashville (USA) to analyse whether these were connected with AR events, while Ryoo et at. (2015) analysed the transport pathways of water vapour associated with AR events that made landfall along the West Coast of the USA between 1997 and 2010. In addition, Rutz et al. (2015) analysed the evolution of ARs over western North America using trajectories released at 950 and 700 hPa within ARs along the Pacific coast. In this case a forward mode was used to study the inland penetration of ARs.

For Europe, Stohl et al. (2008) investigated the remote sources of water vapour forming precipitation in Norway and their link with ARs over a 5-year period. Liberato et al. (2012) showed that the evaporative sources for precipitation falling over Lisbon area, in Portugal, on the heaviest precipitation event occurring there during the twentieth century were distributed over large sectors of the tropical-subtropical North Atlantic Ocean and included a significant contribution from the (sub)tropics. Moreover, Sodemann and Stohl (2013) analysed the origins of moisture and meridional transport in ARs and their association with multiple cyclones in December 2006. Finally, Knippertz and Wernli (2010) presented a Lagrangian climatology of tropical moisture exports to the Northern Hemispheric extra-tropics by analysing forward trajectories leaving a box between 0º and 20ºN for 1979-2001.

These researchers based their results on the use of Lagrangian models, which allow to study the evolution of moisture in the atmosphere along a number of trajectories. The use of Lagrangian models such as FLEXPART (Stohl et al., 1998) can help us to assess the main sources of moisture and its transport within ARs. This Lagrangian model allows us to follow the moisture that reaches a specific region, more specifically making it possible to track changes in the specific humidity along the trajectories over time. By knowing the specific humidity (q) at every time step it is possible identify those particles that lose moisture through precipitation (p), or receive it through evaporation (e). FLEXPART can “transport” these particles backwards or forwards in time using a 3D wind field. The record of evaporation minus precipitation (e-p) provides information on the sources (when evaporation exceeds precipitation) and sinks (when precipitation exceeds evaporation) of moisture.

The Lagrangian methodology of identifying moisture sources based on FLEXPART has been extensively used over the past decade both for regional (e.g., Nieto et al., 2006) and global studies (Gimeno et al., 2010a). The comprehensive review by Gimeno et al. (2012) provides details of the uncertainty and significance of this Lagrangian approach, as well as a comparison with other methods of estimating moisture sources, and the original paper by Stohl et al. (2004) provides further information on the FLEXPART model. Here we are mainly interested in analysing the backward trajectories that arrive in the various regions along the Atlantic coast of Europe where ARs make landfall. The objectives of this work are: 1) to identify the ARs affecting the western European coast between 1979-2012 during the winter half-year (ONDJFM) and, 2) to provide a comprehensive analysis of the areas where the AR moisture uptake is anomalous over the same period for the ARs that reach the different European domains. The added value of the manuscript is mainly twofold: a) firstly the current study is the first to analyse those areas where the moisture uptake is anomalous for the ARs that reach the European coast from a climatological perspective; b) secondly we have made refinements to the AR tracking method introduced by Lavers et al. (2012). In the present version, we use 3 reference meridians rather than a single fixed one for the whole of Western Europe to have a higher accuracy on landfall times and locations (see Sect. 2.1). This is of the utmost importance for analysing the anomaly for the moisture uptake for the ARs based on the use of (E-P), because just a few degrees of difference in the reference meridian longitude may translate into an erroneous detection for any anomalous moisture sources.

The work is organised as follows: we present the datasets and the different methodologies in Sect. 2 while in Sect. 3 we analyse ARs that reach landfall in Europe. The detection of those areas where the moisture uptake is anomalous for ARs that reach Europe is analysed in Sect. 4. Finally, our conclusions are presented in Sect. 5.

2 Methods and Datasets

2.1 Atmospheric River detection

The detection of ARs can be achieved by adopting two very different approaches, namely a) using integrated column water vapour (IWV) (e.g., Ralph et al., 2004; Ralph and Dettinger, 2011), and b) based on vertically integrated horizontal water vapour transport (IVT) (e.g., Zhu and Newell, 1998; Lavers et al., 2012; Ramos et al., 2015). The choice of either of these two approaches is perfectly valid, and will depend on the purpose and location of the study.

In this case we have used the ERA-Interim reanalysis (Dee et al., 2011) with a 0.75º latitude-longitude grid resolution, spanning from 1979-2012 for the winter half-year (October to March, ONDJFM) for the detection of ARs. The variables used at 6-h time steps were the specific humidity, as well as zonal and meridional winds at the 1000, 925, 850, 700, 600, 500, 400 and 300 hPa levels, given that most of the moisture transport is accounted for in these levels.

The AR detection scheme employed (Lavers et al., 2012; Ramos et al., 2015) depends entirely on the vertically integrated horizontal water vapour transport (IVT) and was computed between the 1000 and the 300 hPa levels (equation 1):

$$IVT = \sqrt{\left(\frac{1}{g}\int_{1000hPa}^{300hPa} qu dp\right)^2 + \left(\frac{1}{g}\int_{1000hPa}^{300hPa} qv dp\right)^2}, \quad (1)$$

where *q* is the specific humidity, *u* and *v* are the zonal and meridional layer averaged wind respectively, while *dp* is the pressure difference between two adjacent levels. *g* denotes the acceleration due to gravity.

The identification of ARs is similar to that performed by Lavers and Villarini (2013) for Europe and Ramos et al. (2015) for the Iberian Peninsula, and considers only one reference meridian for the computation of the ARs. In this case we have used three distinct reference meridians (Fig. 1) located at 9.75ºW (meridian 1, just west of both the Iberian Peninsula and Ireland), 4.50ºW (meridian 2, located west of the UK and France), and 5.25ºE (meridian 3, west of Scandinavia). Each different reference meridian (Fig. 1) was further divided into 10º latitudinal sections between 35ºN and 75ºN for the 9.75°W and 4.50ºW reference meridians, and between 50ºN and 70ºN for the 5.25ºE reference meridian, to allow for differences in IVT depending on latitude.

The value for the highest IVT and its respective latitude (IVT threshold) for each meridian was computed as follows: we extracted the maximum IVT at 1200UTC each day for the entire period between 35ºN and 75ºN (for the 9.75ºW and 4.50°W meridians) and between 50ºN and 70ºN (for the 5.25ºE meridian) and sorted these into 10º latitude bins. Following the approach adopted in Lavers et al. (2013), the threshold chosen for each bin corresponds to the 85th percentile of the maximum IVT values included in that bin. The derived thresholds for the different reference meridians and sectors are summarised in Table 1.

Having computed the different thresholds for each reference meridian the following detection scheme was applied for each sector:

a) at each 6-h time step of the dataset (each day has 4 time steps) between 1979 and 2012 over the winter half-year, we compared the IVT values at the grid points for each reference meridian and extracted the maximum IVT value and its location;
b) where the maximum IVT exceeded the local IVT threshold (which depends on both longitude and latitude and was computed for each meridian reference bin (Table 1), this particular grid point was highlighted. We then performed a west/east search to identify the maximum IVT at each longitude and tracked the location for the grid points where the local IVT threshold was exceeded. However, ARs have to extend for at least 1500 km, therefore a minimum length threshold was also imposed. In this case, it corresponded to 30 contiguous longitude points (30*0.75º=22.25º~1600 km, considering that at 50°N the length of a degree of longitude is ~71km) Provided that this condition was fulfilled for a particular time step we considered it to be an AR time step;
c) because we applied the same procedure to all time steps, we obtained all the AR time steps identified for the different reference meridians, but only persistent AR events were retained. For a persistent AR event to occur (Lavers and Villarini 2013; Ramos et al., 2015) a temporal criterion was applied in that 1) it required a persistence of at least 18h (three continuous time steps), and 2) to be independent, two persistent ARs were considered distinct only when they were separated by more than 1 day (four time steps). A spatial criterion was also applied: a movement of not more than 4.5º latitude to the north or south of the initial IVT maximum in a 18h period.

The number of persistent ARs identified for each reference meridian is summarised in Table 1 (last column) and will be discussed in Sect. 3. Given that we are particularly interested in those ARs that have impacts over land we reorganised the previously computed ARs (Fig. 1 and Table 1) into the following 5 new domains shown in Fig. 1 using different coloured solid lines and identified as: 1) *Iberian Peninsula* (red, 9.75ºW; 36ºN – 43.75ºN); 2) *France* (blue, 4.5ºW; 43.75ºN – 50ºN); 3) *UK* (green, 4.5ºW; 50ºN-59ºN); 4) *Southern Scandinavia and the Netherlands* (yellow, 5.25ºE; 50ºN-59ºN) and 5) *Northern Scandinavia* (purple, 5.25ºE; 59ºN – 70ºN). This allows us to use contiguous domains from 36ºN to 70ºN, with domains 3) and 4) only differing in terms of the meridional reference while maintaining the same latitudinal division. This new division will be very helpful in Sect. 4 where the study of the anomalous moisture uptake for ARs will be analysed in greater detail, given that the specific location at which the ARs make landfall is of the utmost importance.

2.2 Lagrangian moisture quantification

The method developed by Stohl and James (2004) allows us to track the atmospheric moisture along Lagrangian trajectories of air parcels in the atmosphere using the FLEXPART v9.0 Lagrangian model. This model simulates the movement of approximately 2.0 million atmospheric parcels every 3 hours. Our global simulation was forced using data ERA-Interim reanalysis data (Dee et al., 2011) from 1979 to 2012. At each initial time this Lagrangian model distributes the air parcels (also namely particles) homogeneously to cover the largest possible volume, always taking the distribution of mass in the atmosphere into account. The FLEXPART model imposes a condition on the mass, which must be constant. The mass takes into account the volume and the density of the air. We use 61 levels in the atmosphere, from 1000 to 0.1 hPa, so the volume of the air parcel varies in accordance with the level concerned: a volume is thus smaller near the surface and larger higher up because the air density is greater near the surface and lower at high altitudes. These particles are then moved using the reanalysis wind field, and in addition turbulence and convection parametrizations are taken in account, always maintaining the consistency of the atmospheric mass distribution (Stohl et al., 1998; Stohl et al., 2005). The meteorological properties of the air parcels, such as specific humidity or temperature among many others, are retained in the outputs of the FLEXPART model, taking into account the ERA-Interim reanalysis input.

The changes in specific humidity (dq) of a particle (with mass m) over time (dt) during its trajectory can be expressed as (equation 2):

$$e - p = m\frac{dq}{dt}, \qquad (2)$$

where (e-p) can be inferred as the freshwater flux in the parcel (the difference between evaporation and precipitation).

The moisture changes (e-p) of all the particles in the atmospheric column over a specified area (A) yields the surface freshwater flux (E-P), where E is the evaporation rate per unit area, and P is the precipitation rate per unit area (equation 3):

$$E - P \approx \frac{\sum_{k=1}^{K}(e-p)}{A}, \qquad (3)$$

where K is the total number of particles in the atmospheric column. Each particle is tracked backwards for a transport time of 10 days, this being the average residence time of water vapour in the atmosphere (Numaguti, 1999).

The different areas where the ARs make landfall are discussed in Sect. 3, while the selection of each European domain where the particles are selected for the backward trajectories (E-P) analyses will be discussed in Sect. 4.

3 Landfall of atmospheric rivers in Europe

The number of ARs for each domain is summarised in Table 1. There were 271 ARs for reference meridian 1, with a maximum of 87 ARs in the 45º-55ºN sector; for reference meridian 2 the total number is 351, with a maximum of 98 ARs observed at latitudes between 55ºN and 65ºN. In the case of reference meridian 3 and given that the ARs come from the Atlantic region, we divided the reference meridian into two sectors (50ºN to 60ºN and 60ºN to 70ºN), with the maximum number of ARs being recorded in the 50ºN-60ºN sectors (100 ARs). The IVT threshold has a maximum around 45ºN and 55ºN for the reference meridians, in good agreement with the results obtained by Lavers and Villarini (2013) near 10ºW. In addition, this maximum is also confirmed by the analysis of the seasonal IVT mean fields, where a maximum is present between 45ºN and 55ºN (not shown).

The number of ARs and the corresponding AR time steps for each new domain are shown in Table 2 and will be analysed in detail in Sect. 4. This varies from 21 ARs (117 time steps) in the Iberian Peninsula domain up to 140 ARs (665 time steps) in the France domain.

This assessment of ARs for the different reference meridians confirms the findings of Lavers and Villarini (2013) that the ARs also strike regions of Europe other than the Iberian Peninsula (Ramos et al., 2015) or the UK (Lavers et al., 2011). In this regard, we are confident that the use of three different meridians of control (9.75ºW, 4.5ºW and 5.25ºE) provides a more precise and robust assessment of all the ARs that make landfall in Europe.

While it can be argued that the overall frequency of ARs is rather low, in fact we are particularly interested in analysing tracking and the anomalous moisture sources for the most intense ARs, i.e., those ARs that are often associated with extreme precipitation events. It has been shown that a large proportion of the most intense precipitation events (and of course their associated floods) in Western Europe are objectively associated with the occurrence of ARs, both in the UK (Lavers et al., 2013) and in the Iberian Peninsula (Ramos et al., 2015). In particular, Lavers and Villarini (2013) showed in their Fig. 3 the number of Top 10 Annual maximum events related to ARs. It is immediately striking that some areas of the Iberian Peninsula, France, UK, and Norway have up to 6 out of 10 top annual maxima associated with ARs. In addition, Ramos et al. (2015) for the Iberian Peninsula showed that ARs play an overwhelming role in the most extreme precipitation days but these decrease in importance for less extreme precipitation days.

The refinements made to the detection scheme for ARs (in the use of three reference meridians regrouped into five sub-domains in terms of their geographical relevance) as introduced by Lavers et al. (2012), were intended to improve AR detection and allow us to obtain more precise locations for AR landfalls. To analyse whether these refinements actually improve AR detection, the number of Top 10 annual maxima precipitation events (for the extended winter months, i.e., ONDJFM) related to ARs were computed. To this end, the annual maxima were computed for each calendar year (only for the extended winter months) from 1979 to 2012 at each grid point (E-OBS, at 0.25º resolution, Haylock et al., 2008). The results obtained (supplementary material Fig. S1) show that there is an improvement in the relationship between ARs and annual maxima for France, Belgium, Germany and the Scandinavian countries compared to the results of Lavers and Villarini (2013), in their Fig. 3.

In order to track the path of the ARs, we computed the maximum longitudinal IVT for each AR, in order to obtain a preliminary estimate of the position of the ARs in the North Atlantic Ocean. For each new domain, we computed the median, 90th, and 10th percentile of the maximum IVT positions of the different ARs along their first-guess trajectories and the results are presented in Fig. 2. The use of the 90th and 10th percentiles allows us to visualise the spread of the positions of the vast majority of the ARs throughout the North Atlantic basin associated with each domain.

Regarding the Iberian Peninsula (Fig. 2a), the median position of the ARs is mainly zonal, with a small WSW component, while their spatial dispersion is quite high, particularly as we move away from the landfall area. This WSW component is in line with the results obtained by Ramos et al. (2015), where a positive anomaly of Sea Level Pressure is found to the south of Portugal when the ARs make landfall in the Iberian Peninsula.

In the cases of France and the UK (Fig. 2b), the paths and dispersions are similar with respect to the median path of the ARs, especially on the Eastern North Atlantic. The main differences are closer to the two domains, namely: 1) a more zonal path associated with the France domain, while for the UK its path near the reference meridian is clearly more SW-NE oriented, and 2) the dispersion of the AR paths is higher for the UK domain than for the France domain, particularly to the west of 40ºW. The results for the UK confirm those obtained by Lavers et al. (2011), although here we have used the full climatology where Lavers et al. (2011) only analysed the AR paths for selected cases. Concerning the last two domains (Fig. 2c), the results are very similar to those obtained for the France and UK domains, i.e., most ARs show a strong SW-NE orientation, particularly to the east of 40ºW for those ARs that arrive in the north Scandinavian domain. In addition, the dispersion of the paths in these two domains is relatively high compared with the other three domains.

These five new domains (Fig. 1) are those that will be used in the computation of the moisture transport for the ARs that make landfall over the western coasts of the European domains analysed.

4 Atmospheric rivers and anomalous moisture uptake

The use of the integrated horizontal flux transport (IVT) is an effective Eulerian approach for studying the temporal variability of moisture flows for specific locations around the globe, and is therefore widely used in the identification of ARs. However, this Eulerian perspective is not suitable for finding sources of moisture, and of course it is impossible to use it compute where the uptake of moisture to the AR is, given that the method is not able to follow any specific “particle” transported by the ARs. To illustrate the difference between the use of the IVT and the information that can be extracted from FLEXPART, we provide in Fig.3 an example of a particular AR that occurred on 14 December 1981 at 00UTC, which reached the Iberian Peninsula. Fig. 3a shows the sources of moisture (E-P)>0 computed for 10 days back in time (reddish colours). Three areas clearly emerge as sources: one located to the west of the Iberian Peninsula near the coast, and two larger ones located in the central and western Atlantic. In Fig. 3b we show the IVT field for the same day and the maximum edge of the IVT denoted by a black line and used in this study to detect ARs, together with a red contour delimiting the sources of moisture in Fig 3a. It can clearly be seen that the moisture sources and the IVT maximum are not coincident. When we analyse either the IVT maximum or the IVT field, we only reveal a snapshot of the integrated horizontal flux transport for that specific time-step, and not the path of the air masses. This indicates neither where the moisture comes from, nor where the moisture uptake is anomalous during the previous days of the AR, which is one of the objectives of this analysis.

The use of Lagrangian models such as FLEXPART allows us to study air parcels as they move through space and time, i.e., their trajectory, and also allows us to characterise accurately the history of the air parcels (e.g., their specific humidity) that arrive at a specific site. The use of Lagrangian models was shown to be a worthwhile and important tool for analysing the moisture sources in a case study of ARs in Norway (Stohl et al., 2008) and in Portugal (Liberato et al. 2012). In the latter case the methodology has been applied over different accumulated periods (for 1 to 3, 3 to 5 and 5 to 10 days) allowing also to identify the relative importance of the several moisture sources contribution over time. Our use of FLEXPART simulations and the computation of (E-P) is intended to help us locate the origin of the anomalous moisture uptake associated with ARs reaching the Atlantic European coast for all the systems detected and from a climatological point of view. It is important to note that an AR transports a large amount of moisture that often reaches a continental area. This moisture must necessarily be available for transport in the atmosphere. Therefore, it must be evaporated and accumulated in certain areas during the days prior to the intense track of the AR. The existence of an intense flux is important but not sufficient, in that an intense anomalous quantity of moisture must be available for the AR to occur. Therefore, in this research we detect (for the 10 days prior to the AR reaching landfall) where the moisture uptake to the atmosphere is anomalous.

The backward trajectory analyses were performed for air particles residing over the area 5° to the west of the AR detection meridian reference (Table 3): e.g., for the Iberian Peninsula region it included particles located inside a rectangle (covering an area between 9.75ºW and 4.75ºW and from 36ºN to 43.75ºN) and tracked backwards for 10 days at 6-hour intervals (a total of 40 time steps).

We computed the uptake of moisture for all individual ARs at all time steps, retaining only positive values of (E-P) every 6 hours during the 10-day back trajectories (40 time steps). For instance, there are 117 cases for the Iberian Peninsula, so we computed 117 fields of (E-P)>0, and the same for the other domains. To check whether these areas (where the ARs take on moisture) differ from the climatology, we computed for each AR the anomaly between (E-P)>0 of the ARs and the ‘climatology’ for the corresponding AR dates. The ‘climatology’ at this point corresponded to the same (Julian) time step but for all 33 years of the study (retaining again only the positive values of (E-P) for each 6-h time step). For the example given in Fig. 3, if an AR existed on 14 December 1981 00UTC, we computed the anomaly between a) (E-P>0) on 14 December 1981 00UTC and b) (E-P)>0 for all time steps of 14 December 00UTC, in other words, (E-P)>0 for the corresponding day for the 33 years of the entire period. We then computed the anomaly for this particular case (14 December 1981 00UTC) using the difference between b) and a). The climatology and the anomaly for each domain, denoted by $(E\text{-}P)_{Cli}>0$

and $(E\text{-}P)_{An}>0$ in Fig.4, corresponds to the mean values for all the respective ARs. A representation of the fields of $(E\text{-}P)_{Cli}>0$ and $(E\text{-}P)_{An}>0$ for all the five regions studied is provided in Fig.4 (left panel) and Fig.4 (right panel), respectively. Moreover, the anomalous moisture of the sources are only shown for the areas that are statistically significant at the 90% level, applying a T-student test to the (E-P)>0 for all the ARs and the climatology (Table 4). In general, for all regions the major anomalous uptake of moisture (hereafter AUM) extends along the subtropical north Atlantic (from the Tropic of Cancer to 35°N according to the definition of the American Meteorological Society), from the Gulf Stream Current, just off the Florida Peninsula (to the north of 20ºN), to each sink region, being further to the south (clearly subtropical) on the western basin of the North Atlantic Ocean and reaching extra-tropical latitudes on the eastern basin coast. Moreover, the nearest coast to each sink region always appears as a local maximum of AUM (e.g., see the southern Iberian Peninsula coast or the Bay of Biscay in France). The Norwegian Sea acts as a more important AUM because the region analysed is located at higher latitudes, and is a maximum for the north Scandinavia region.

The distribution of the particle density used to compute the AUM (using a 5º by 5º grid cell) for each domain was also computed. In the supplementary material Fig. S2 shows how many times a parcel (in percentage terms) contributes to the $(E\text{-}P)_{An}>0$ field. In addition, one must be aware that the areas of maximum density of the parcels may (or may not) correspond to areas of maximum anomalies and *vice versa*, because a grid cell can contribute many times but its AUM contribution could be less than that of others with a lower AUM density.

The importance of the North Atlantic Ocean as a source of moisture for some regions of Europe has already been noted in previous studies. In a complete moisture source catalogue for important climate regions, Castillo et al. (2014) showed that for Southern Europe (including our Iberian Peninsula and France domains) and Northern Europe (UK, Southern Scandinavia and the Netherlands, and Northern Scandinavia), the dominant source of moisture is the Northern Atlantic, with a strong signal over the Norwegian Sea when northern continental areas were analysed. Studies focused on specific regions also found similar results, for instance Gimeno et al. (2010b) and Drumond et al. (2011) for the Iberian Peninsula, or studies of European regions at higher latitudes (Nieto et al., 2007; Sodemann et al., 2008) revealed the importance of the Atlantic source. Interestingly, in almost all these studies the authors pointed to the effects of ARs as the major moisture transport mechanism from the subtropical Atlantic. In this work, the key novelty is that we show those regions where the moisture uptake is anomalous and significant when an AR occurs.

We are particularly interested in understanding which regions with higher AUM (depicted in Fig. 4 left panel) are reinforced during ARs associated with each of the five different domains. These reinforced sectors are identified in yellowish and reddish colours in maps of $(E\text{-}P)_{An}$ (Fig. 4, right panel). Overall, the largest anomalies are detected in the middle of the Northern Atlantic, between 20ºN and 40ºN, with a slight northward movement when the sink region is positioned at higher latitudes. These results confirm that part of the excess of moisture transported by ARs vs the climatology comes from tropical latitudes (south of the Tropic of Cancer, 23.43ºN), but the bulk of the additional amount provided by the ARs is obtained from subtropical ocean areas (i.e., those between the Tropic of Cancer and 35ºN). The most notable anomaly is detected for the Iberian Peninsula, followed by Southern Scandinavia and the Netherlands domain, and the lowest is for the Northern Scandinavia domain. Each domain shows differences in values of $(E\text{-}P)_{An}>0$ in both latitude and longitude. To understand these patterns rather better we quantified the anomaly values every 10° between 70ºN and 5ºN and between 10ºW and 60ºW.

Fig. 5 shows the different latitudinal sections for all the studied regions, in which values over the 90th percentile of the anomaly (Table 4) are highlighted using a bold line. We refer to these values to compare the five domains of study. In general, there is a longitudinal southern shift of the anomaly, which is a common feature for all the regions. So for instance, for Northern Scandinavia (purple line) the anomalous uptake of moisture at 10ºW occurs mostly between 60-48ºN, while at 60ºW it occurs predominantly between 40-30ºN; whereas for the Iberian Peninsula (IP, red line) at 10ºW the anomalous uptake occurs mainly in a band between 43-33ºN, and at 60ºW it is particularly intense between 36-21ºN. The Iberian Peninsula shows the highest values of AUM for all the latitudes and is the region where the anomalous moisture uptake occurs furthest south, with local maxima partially over tropical areas. Because the region is positioned more to the North, the tropical AUM tends to be lower, but the subtropical source still dominates, particularly at central and western longitudes. In the supplementary material Fig. S3 is included to complement the information given in Fig. 5, but showing the same results for each individual domain.

To understand more about the effect of ARs over the European domains we checked whether those areas with significant AUM contribute to a significant increase in precipitation. Because FLEXPART can be run in forward mode we looked for the sinks for those air parcels (particles) that leave a particular area, using the AUM regions (those in Fig. 3 right panel) to compute the precipitation (as E-P<0) over each target domain. We computed (E-P)<0 values for the climatological period ($(E\text{-}P<0)_{Clim}$) and only for the AR days ($(E\text{-}P<0)_{AR}$). The results show that the AUM areas associated with ARs support sufficient moisture to increase the precipitation (Table 5). The ratio between the climatology and the AR values provides evidence of an increase ranging from 1.26 times as much precipitation in the UK to 3 times more in the Iberian Peninsula.

It is important to place these results in the light of recent works dealing with the origin of moisture in ARs. Sodemann and Stohl (2013) showed that in December 2006 several ARs reached from the subtropics to high latitudes, inducing precipitation over western Scandinavia. The sources and transport of water vapour in the North Atlantic storm track during that month were examined, and they reveal that the ARs were composed of a sequence of meridional excursions of water vapour. Different moisture sources were found: 1) in cyclone cores, the rapid turnover of water vapour by evaporation and condensation were identified, leading to a rapid assimilation of water from the underlying ocean surface; 2) in the regions of long-range transport, water vapour tracers from the southern edges of the mid-latitudes and subtropics dominated over local contributions. Our results generalize for all the domains previous findings of Liberato et al. (2012) obtained for a case study for Portugal, confirming the presence of extended source areas that support anomalous moisture uptake (tropical and subtropical) for all the domains, with the highest anomalies being found for the Iberian Peninsula and the UK. Because ARs are always dynamically coupled to cyclones, Sodemann and Stohl (2013) also analyse in their study the change in moisture composition in the vicinity of the cyclone responsible for the intense events over western Scandinavia. This fact may be better corroborated in future work by using the long database of ARs for all European coastal domains. In any case, our results also suggest contributions from nearby sources of anomalous moisture uptake associated with the ARs. According to Sodemann and Stohl (2013), this may be due to the rapid turnover of water vapour by evaporation and condensation, leading to the rapid assimilation of water from the underlying ocean surface near the cyclone cores.

We acknowledge the scepticism of some authors regarding the far-reaching origin of moisture considered to contribute to the ARs. Dacre et al. (2015) considered a selected number of cases of water vapour transport associated with North Atlantic extra-tropical cyclones in winter. The authors inferred that AR moisture originates mostly from the water vapour in the cyclone’s warm sector, and not that much from the long-distance transport of water vapour from the subtropics. Our long term $(E\text{-}P)>0$ analysis shows that for the ARs that landfall on the western European coast, the anomalous moisture linked with the ARs comes mainly from subtropical areas and, to a lesser extent, from mid-latitudes. In addition, a small anomalous moisture uptake has also been found in the tropical zone. Garaboa-Paz et al. (2015), using Lagrangian Coherent Structures (LCSs), showed for two AR case studies that the passive advection of water vapour in the AR from tropical latitudes is possible.

5 Conclusions

We have described our innovative study related to the anomalous uptake of moisture for ARs that reach different western European domains in the winter half-year (ONDJFM). To achieve this goal, we used an objective AR detection scheme (Lavers et al., 2012; Ramos et al., 2015) that depends entirely on the vertically integrated horizontal water vapour transport (IVT). In order to ensure that the AR detection is performed as close to the coast as possible, this analysis was applied to 3 different reference meridians (9.75ºW, 4.50ºW and 5.25ºE) divided into 10º sectors between 35ºN and 75ºN. The use of 3 different reference meridians represents a refinement to the approach of Lavers and Villarini (2013), who only used the 10ºW meridian reference. Because we are mostly interested in those ARs that make landfall in western Europe and over land, we regrouped the previously computed ARs (Fig. 1 and Table 1) into the following 5 new domains (Fig. 1): 1) *Iberian Peninsula* (9.75ºW; 36ºN – 43.75ºN); 2) *France* (4.5ºW; 43.75ºN – 50ºN); 3) *UK* (4.5ºW; 50ºN-59ºN); 4) *Southern Scandinavia and the Netherlands* (5.25ºE; 50ºN-59ºN) and 5) *Northern Scandinavia* (5.25ºE; 59ºN – 70ºN).

The number of ARs found shows a latitudinal dependence, with the highest values being recorded for the three meridional references 9.75ºW, 4.50ºW and 5.25ºE are 45ºN - 55ºN, 35ºN - 45ºN and 50ºN - 60ºN respectively. We then considered only those ARs that made landfall in Western Europe over land into the new domains, where the French (140 ARs) and Southern Scandinavia and the Netherlands (90 ARs) domains showed the highest values, while the Iberian Peninsula (21) domain recorded the lowest value.

The Lagrangian perspective of this work can help provide additional input regarding the effective moisture sources associated with most of the ARs that reach Europe. To achieve this objective, we detected those areas where the moisture uptake to the atmosphere occurs in an anomalous way. The computation of positive values of (E-P) every 6 hours for each AR for 10 days of transport was undertaken, taking into account the air particles residing over the 5 degrees west of the ARs detection meridian reference mentioned above and shown in Table 3. This amount was computed for all the ARs that reached a continental domain and was compared with the climatology. We have therefore shown in this paper the anomalous uptake of moisture (here termed the AUM) areas for the ARs.

The near-surface wind speed and the near-surface atmospheric specific humidity, together with the SST, are bound to play a major role in the process of moisture uptake over the Oceans (Gimeno et al., 2012). Therefore, despite not analysing the role of SST in the present study, we can nevertheless speculate the possibility of positive anomalies of sea surface temperature influencing the interannual variably of the ARs. Future studies of the SST variability and its influence over the ARs should be considered in order to understand this relationship better.

The most important results obtained can be summarised as follows:

- In general, for all the regions, the major AUM areas extend along the subtropical North Atlantic, from the Florida Peninsula (north of 20ºN) to each sink region. However, the mid-latitude also plays an important role, with the coastal area nearest to each sink region always appearing as a local maximum of AUM.
- The Atlantic subtropical AUM source is reinforced during ARs where the major uptake anomalies are detected in the middle of the Northern Atlantic, between 20ºN and 40ºN, with a slight northward movement when the sink region is positioned at higher latitudes.
- The most notable anomaly of moisture uptake is detected for the Iberian Peninsula, followed by the Southern Scandinavia and the Netherlands domains, with the lowest for the Northern Scandinavia domain.

To conclude, we have shown that the main anomalous uptake of moisture areas associated with the ARs that strike Western Europe coast are located over subtropical latitudes. For the southern domains one must be also be aware of the presence of a tropical AUM area. Near the sink continental areas, extra-tropical areas with anomalous uptake of moisture are also apparent, confirming the local transport produced by the nearby ocean.

Acknowledgements

Alexandre M. Ramos was supported through a postdoctoral grant (SFRH/BPD/84328/2012) from the Fundação para a Ciência e a Tecnologia (FCT, Portuguese Science Foundation). This work also was partially supported by FEDER funds through the COMPETE (Programa Operacional Factores de Competitividade) Programme and by national funds through FCT through project STORMEx FCOMP-01-0124-FEDER-019524 (PTDC/AAC-CLI/121339/2010). Raquel Nieto acknowledges funding by the Spanish MINECO within project TRAMO and the Galician Regional Government (Xunta) within project THIS, both co-funded by FEDER.

References

Bao, J-W., Michelson, S. A., Neiman, P. J., Ralph, F. M., and Wilczak, J. M.: Interpretation of enhanced integrated water vapor bands associated with extratropical cyclones: Their formation and connection to tropical moisture, Mon. Weather Rev., 134, 1063–1080, 2006.

Castillo, R., Nieto R., Drumond, A., and Gimeno, L.: Estimating the temporal domain when the discount of the net evaporation term affects the resulting net precipitation pattern in the moisture budget using a 3-D Lagrangian approach, PLoS ONE, 9(6), doi:10.1371/journal.pone.0099046, 2014.

Couto, F.T., Salgado, R., Costa, M.J.: Analysis of intense rainfall events on Madeira Island during the 2009/2010 winter, Nat. Hazards Earth Syst. Sci. 12, 2225–2240, doi: 10.5194/nhess-12-2225-2012, 2012.

Couto, F.T., Salgado, R., Costa, M.J., Prior, V.: Precipitation in the Madeira Is- land over a 10-year period and the meridional water vapour transport during the winter seasons. Int. J. Climatol. 35, 3748–3759, http://dx.doi.org/10.1002/joc.4243, 2015.

Dettinger, M., Ralph, F. M., Das, T., Neiman, P. J., and Cayan, D. R.: Atmospheric Rivers, Floods and the Water Resources of California, Water, 3, 445-478, 2011.

Dettinger, M., Ralph, F. M., and Lavers, D.: Setting the stage for a global science of atmospheric rivers, Eos, 96, doi:10.1029/2015EO038675, 2015.

Dee, D. P., with 35 co-authors.: The ERA-Interim reanalysis: configuration and performance of the data assimilation system, Quart. J. R. Meteorol. Soc., 137, 553-597, 2011.

Dacre, H., Clark, P., Martinez-Alvarado, O., Stringer, M., and Lavers, D.: How do atmospheric rivers form?, Bull. Am. Met. Soc., doi:10.1175/BAMS-D-14-00031.1, in press, 2015.

Drumond, A., Gimeno, L., and Nieto, R.: On the contribution of the Tropical Western Hemisphere Warm Pool source of moisture to the northern hemisphere precipitation through a lagrangian approach, J. Geophys. Res, 116, D00Q04, doi:10.1029/2010JD015397, 2011.

Ferreira, J.A., Liberato, M.L.R., Ramos, A.M.: On the relationship between atmospheric water vapour transport and extra-tropical cyclones development. Physics and Chemistry of the Earth. doi: 10.1016/j.pce.2016.01.001, 2016.

Garaboa-Paz, D., Eiras-Barca J., Huhn F., Pérez-Muñuzuri, V.: Lagrangian coherent structures along atmospheric rivers. Chaos 25, 063105; doi: 10.1063/1.4919768, 2015

Gimeno, L., Stohl, A., Trigo, R.M., Domínguez, F., Yoshimura, K., Yu, L., Drumond, A., Durán-Quesada, A.M., Nieto R.: Oceanic and Terrestrial Sources of Continental Precipitation, Reviews of Geophysics, 50, RG4003, doi:10.1029/2012RG000389, 2012.

Gimeno, L., Drumond, A., Nieto, R., Trigo, R. M., Stohl, A.: On the origin of continental precipitation, Geophys. Res. Lett., 37, doi: 10.1029/2010GL043712, 2010.

Gimeno, L., Nieto, R., Trigo, R. M., Vicente, S., and Lopez-Moreno, J. I.: Where does the Iberian Peninsula moisture come from? An answer based on a Largrangian approach, Journal of Hydrometeorology, doi: 10.1175/2009JHM1182.1, 2010.

Gimeno, L., Nieto, R., Vázquez, M., and Lavers, D.A.: Atmospheric rivers: a mini-review, Front. Earth Sci., 2:2. doi: 10.3389/feart.2014.00002, 2014.

Haylock, M. R., Hofstra, N., Klein Tank, A. M. G., Klok, E. J., Jones, P. D. and New, M.: A European daily high-resolution gridded data set of surface temperature and precipitation for 1950–2006, J. Geophys. Res., 113, D20119, doi:10.1029/2008JD010201, 2008

Knippertz, P., and Wernli, H.: A Lagrangian Climatology of Tropical Moisture Exports to the Northern Hemispheric Extratropics, J. Climate, 23, 987–1003, 2010.

Lavers, D. A., Allan, R. P., Wood, E. F., Villarini, G., D. J., Brayshaw, and Wade, A. J.: Winter floods in Britain are connected to atmospheric rivers, Geophys. Res. Lett., 38, L23803, doi:10.1029/2011GL049783, 2011.

Lavers, D. A., and Villarini, G.: The nexus between atmospheric rivers and extreme precipitation across Europe, Geophys. Res. Lett., 40, 3259–3264, 2013.

Lavers, D. A., Villarini, G., Allan, R. P., Wood, E. F., and Wade, A. J.: The detection of atmospheric rivers in atmospheric reanalyses and their links to British winter floods and the large-scale climatic circulation, J. Geophys. Res., 117, D20106, doi:10.1029/2012JD018027, 2012.

Liberato, M. L. R., Ramos, A. M., Trigo, R. M., Trigo, I.F., Durán-Quesada, A. M., Nieto, R., and Gimeno, L.: Moisture Sources and Large-Scale Dynamics Associated With a Flash Flood Event, in Lagrangian Modeling of the Atmosphere (eds J. Lin, D. Brunner, C. Gerbig, A. Stohl, A. Luhar and P. Webley), American Geophysical Union, Washington, D. C., doi: 10.1029/2012GM001244, 2012.

Moore, B. J., Neiman, P. J., Ralph, F. M., and Barthold, F. E.: Physical processes associated with heavy flooding rainfall in Nashville, Tennessee, and vicinity during 1–2 May 2010: The role of an atmospheric river and mesoscale convective systems, Mon. Wea. Rev., 140, 358–378, 2012.

Neiman, P. J., Ralph, F. M., Wick, G. A., Lundquist, J. D., and Dettinger, M. D.: Meteorological characteristics and overland precipitation impacts of atmospheric rivers affecting the West Coast of North America based on eight years of SSM/I satellite observations, J. Hydrometeorol., 9(1), 22–47, 2008.

Nieto, R., and Gimeno, L.: Atmospheric transport towards the Iberian Peninsula in the range 3-10 days. Sources of middle-lived pollutants and aerosols, Scientific World J., 6, 1041-1047, doi:10.1100/tsw.2006.208, 2006.

Nieto, R., Gimeno, L., Gallego, D., Trigo, R.M.: Identification of major sources of moisture and precipitation over Iceland, Meteorologische Zeitschrift,16(1), 37-44, 2007.

Numaguti, A.: Origin and recycling processes of precipitating water over the Eurasian continent: Experiments using an atmospheric general circulation model, J. Geophys. Res., 104, 1957-1972, 1999.

Ralph, F. M., Coleman, T., Neiman, P. J., Zamora, R. J., Dettinger, M. D.: Observed Impacts of Duration and Seasonality of Atmospheric-River Landfalls on Soil Moisture and Runoff in Coastal Northern California, J. Hydrometeor., 14, 443–459, 2013.

Ralph, F. M., and Dettinger, M. D.: Storms, floods, and the science of atmospheric rivers, Eos Trans. AGU, 92(32), 265, 2011.

Ralph, F. M., Neiman, P. J. and Wick, G. A.: Satellite and CALJET aircraft observations of atmospheric rivers over the eastern North Pacific Ocean during the winter of 1997/98, Mon. Weather Rev., 132, 1721–1745, 2004.

Ramos, A. M., Trigo, R. M., Liberato, M. L. R., and Tome, R.: Daily precipitation extreme events in the Iberian Peninsula and its association with Atmospheric Rivers, J. Hydrometeorol., 16, 579–597, doi: 10.1175/JHM-D-14-0103.1, 2015.

Stohl, A., Forster, C., Frank, A., Seibert, P., Wotawa ,G.: Technical Note : The Lagrangian particle dispersion model FLEXPART version 6.2. Atmos. Chem. Phys., 5, 2461-2474, 2005.

Stohl, A., Forster, C., and Sodemann, C.: Remote sources of water vapor forming precipitation on the Norwegian west coast at 60°N: A tale of hurricanes and an atmospheric river, J. Geophys. Res., 113, D05102, 2008.

Stohl, A., Hittenberger, M., and Wotawa, G.: Validation of the Lagrangian particle dispersion model FLEXPART against large-scale tracer experiment data, Atmos. Environ., 32, 4245–4264, 1998.

Stohl, A., and James, P. A.: Lagrangian Analysis of the atmospheric branch of the global water cycle. Part I: Method description, validation, and demonstration for the August 2002 flooding in Central Europe, J. Hydrometeor., 5, 656-678, 2004.

Sodemann, H., and Stohl, A.: Moisture Origin and Meridional Transport in Atmospheric Rivers and Their Association with Multiple Cyclones. Mon. Wea. Rev., 141, 2850–2868, 2013

Sodemann, H., Schwierz, C., and Wernli, H.: Interannual variability of Greenland winter precipitation sources: Lagrangian moisture diagnostic and North Atlantic Oscillation influence, J. Geophys. Res., 113, D03107, doi:10.1029/2007JD008503, 2008.

Trigo, R. M., Varino, F., Ramos, A. M., Valente, M. A., Zêzere, J. L., Vaquero, J. M., Gouveia, C. M., and Russo, A.: The record precipitation and flood event in Iberia in December 1876: description and synoptic analysis, Front. Earth Sci. 2:3. doi: 10.3389/feart.2014.00003, 2014

Zhu, Y., and Newell, R. E.: A proposed algorithm for moisture fluxes from atmospheric rivers, Mon. Weather Rev., 126(3), 725–735, 1998.

Tables

Table 1. The vertically integrated horizontal water vapour transport (IVT) threshold and the number of persistent atmospheric rivers detected for each different reference meridian

	Sector	**IVT threshold ($kg\ m^{-1}\ s^{-1}$)**	**Number of AR**
Reference meridian 1 **(9.75ºW)**	35ºN - 45ºN	621.7048	79
	45ºN - 55ºN	691.5456	87
	55ºN - 65ºN	614.4121	70
	65ºN - 75ºN	453.4208	35
Reference meridian 2 **(4.50ºW)**	35ºN - 45ºN	527.9475	113
	45ºN - 55ºN	637.2342	94
	55ºN - 65ºN	544.0915	98
	65ºN - 75ºN	439.4734	46
Reference meridian 3 **(5.25ºE)**	50ºN - 60ºN	524.1678	100
	60ºN - 70ºN	468.0643	80

Table 2. The new defined Atmospheric Rivers landfall domains and the corresponding number of Atmospheric Rivers and the respective number of time steps.

ARs domains	Number of ARs	Number of ARs time steps
1) Iberian Peninsula 9.75ºW; 36ºN – 43.75ºN	21	117
2) France 4.5ºW; 43.75ºN – 50ºN	140	665
3) UK 4.5ºW; 50ºN-59ºN	74	343
4) Southern Scandinavia and The Netherlands 5.25ºE; 50ºN-59ºN	90	423
5) Northern Scandinavia 5.25ºE; 59ºN – 70ºN	83	317

Table 3. (E-P) backward trajectories regions where the computation is made for all the air parcels inside it.

ARs domains	Latitude and Longitude limits
1) Iberian Peninsula	9.75ºW – 4.75ºW ; 36ºN – 43.75ºN
2) France	4.5ºW – 0.5ºE ; 43.75ºN – 50ºN
3) UK	4.5ºW – 0.5ºE ; 50ºN – 59ºN
4) Southern Scandinavia and The Netherlands	5.25ºE – 10.25ºE ; 50ºN – 59ºN
5) Northern Scandinavia	5.25ºE – 10.25ºE ; 59ºN – 70ºN

Table 4. Percentile 90th for the anomaly values of (E-P) > 0 field [$(E\text{-}P)_{An}$] for each studied domain and longitude (in mm/day):

	Iberian Peninsula	**France**	**UK**	**Southern Scandinavia and the Netherlands**	**Northern Scandinavia**
10ºW	0.45	0.40	0.50	0.55	0.41
20ºW	0.77	0.56	0.69	0.73	0.53
30ºW	0.82	0.69	0.90	0.86	0.63
40ºW	0.99	0.85	0.93	0.90	0.62
50ºW	0.98	0.81	0.83	0.80	0.56
60ºW	1.06	0.79	0.64	0.71	0.52

Table 5. The contribution of the different moisture sources to the precipitation derived from FLEXPART, computed as E-P<0 (P_{FLEX}), over the analysed 5 domains for the climatological period (P_{FLEX}Clim) and for the ARs days (P_{FLEX}AR). The ratio between the two is also shown.

Domain	P_{FLEX}Clim **(mm/day)**	P_{FLEX}AR **(mm/day)**	P_{FLEX}AR/ P_{FLEX}Clim
1) Iberian Peninsula	255.85	788.14	3.07
2) France	360.94	779.01	2.16
3) UK	561.61	709.86	1.26
4) Southern Scandinavia and the Netherlands	616.42	829.89	1.34
5) Northern Scandinavia	601.35	871.06	1.44

Figure Captions

Figure 1. a) Location of the three different reference meridians and sectors in Europe used for the computation of the Atmospheric Rivers. b) The new defined Atmospheric River landfall domains: Iberian Peninsula (red), France (blue), UK (green), South Scandinavia and the Netherlands (yellow) and North Scandinavia (purple).

Figure 2. The median position (coloured line) and the respective 90^{th} and 10^{th} percentiles (dashed lines) of the Atmospheric River path along the North Atlantic Ocean before arriving in each studied domain: a) Iberian Peninsula (red), b) France (blue) and UK (green) and c) Southern Scandinavia and the Netherlands (yellow) and Northern Scandinavia (purple).

Figure 3. a) The moisture sources (E-P>0) computed for 10 days for an AR making landfall in the Iberian Peninsula on 14 December 1981 at 00UTC. b) The vertically integrated horizontal water vapour transport (IVT) field for 14 December 1981 at 00UTC and the location of the IVT maxima (black line). The moisture sources detected in a) are also plotted using red contours.

Figure 4. For each studied sink domain (Iberian Peninsula, France, UK, Southern Scandinavia and the Netherlands, and Northern Scandinavia) for wintertime from 1979 to 2012: Left: Mean value of the (E − P) > 0 field $[(E\text{-}P)_{Cli}]$, backward integrated over a 10 day period. Right: (E − P) > 0 anomaly field for AR days $[(E\text{-}P)_{An}]$. Units in mm/day. Regarding the anomaly fields only the results that are statistically significant at the 90% level are shown. The Tropic of Cancer parallel (23.43ºN) and the 35ºN parallel are also shown.

Figure 5. Longitudinal cross section of the anomaly values of (E-P) > 0 field $[(E\text{-}P)_{An}]$ for each studied domain: Iberian Peninsula (red line), France (blue), UK (green), Southern Scandinavia and the Netherlands (yellow), and Northern Scandinavia (purple). The bold line shows those values over the 90^{th} percentile of each series (values shown in Table 4). Units in mm/day. The Tropic of Cancer parallel (23.26ºN) and the 35ºN parallel are also shown.

Supplementary Material Figure Captions

Figure S1. The number of Top 10 annual maxima precipitation events (for the extended winter months) related to Atmospheric Rivers

Figure S2. Track density (%) of the air parcels used to compute the anomalous moisture uptake (at a 5º by 5º grid cell) for a) Iberian Peninsula, b) France, c) UK, d) South Scandinavia and the Netherlands, and e) North Scandinavia.

Figure S3. Longitudinal cross section of the anomaly values of (E-P) > 0 field $[(E\text{-}P)_{An}]$ for each studied domain every 10 degrees: 10°W (red line), 20°W (orange), 30°W (green), 40°W (yellow), 50°W (blue), and 60°W (purple). The bold line shows those values over the 90th percentile of each series (values shown in Table 4). Units in mm/day.

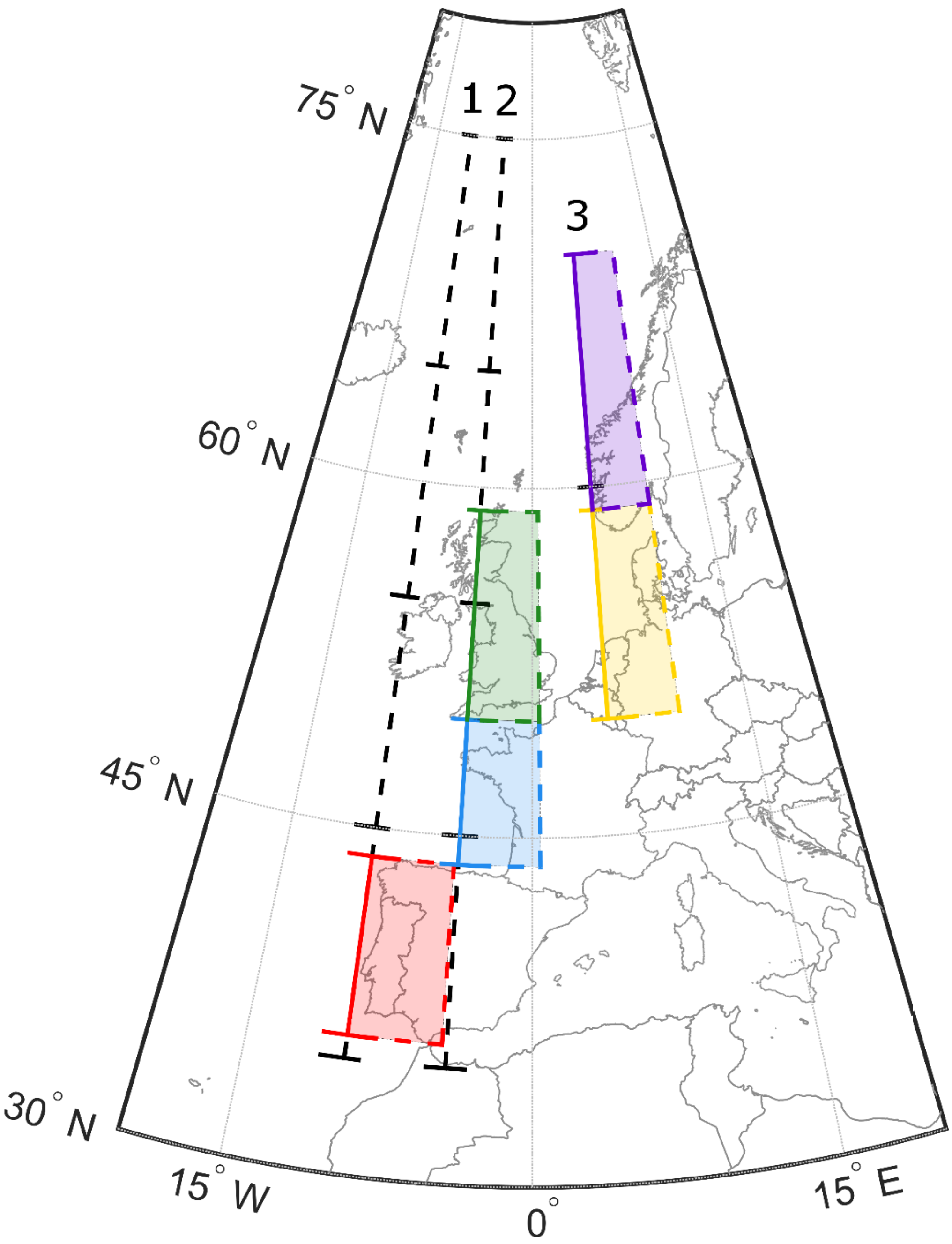

Figure 1.

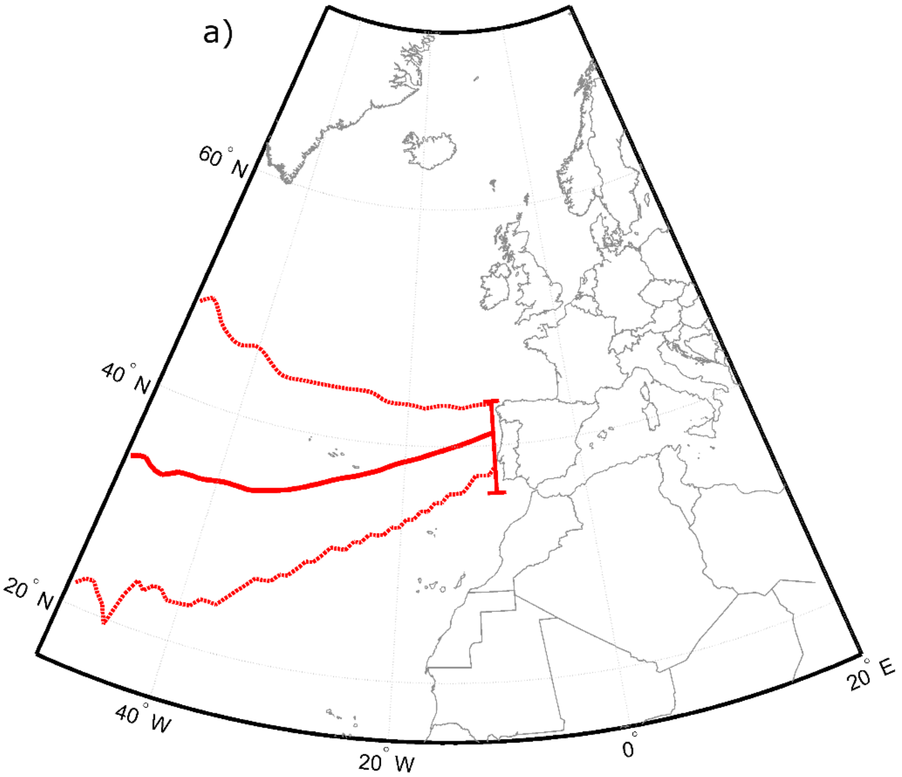
a)
60° N
40° N
20° N
40° W
20° W
0°
20° E

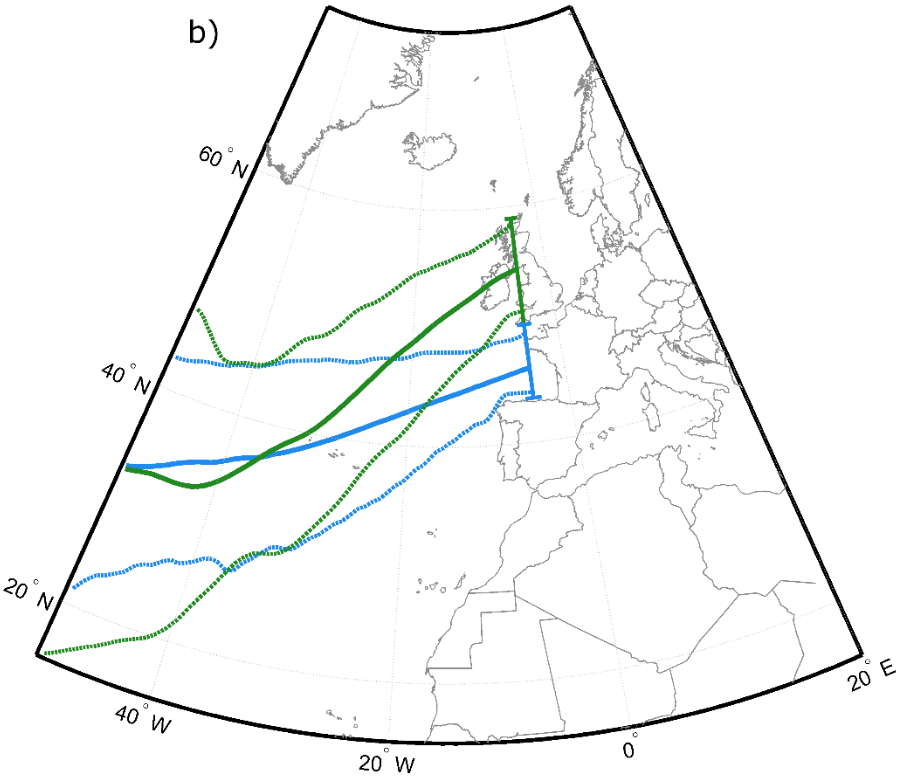
b)
60° N
40° N
20° N
40° W
20° W
0°
20° E

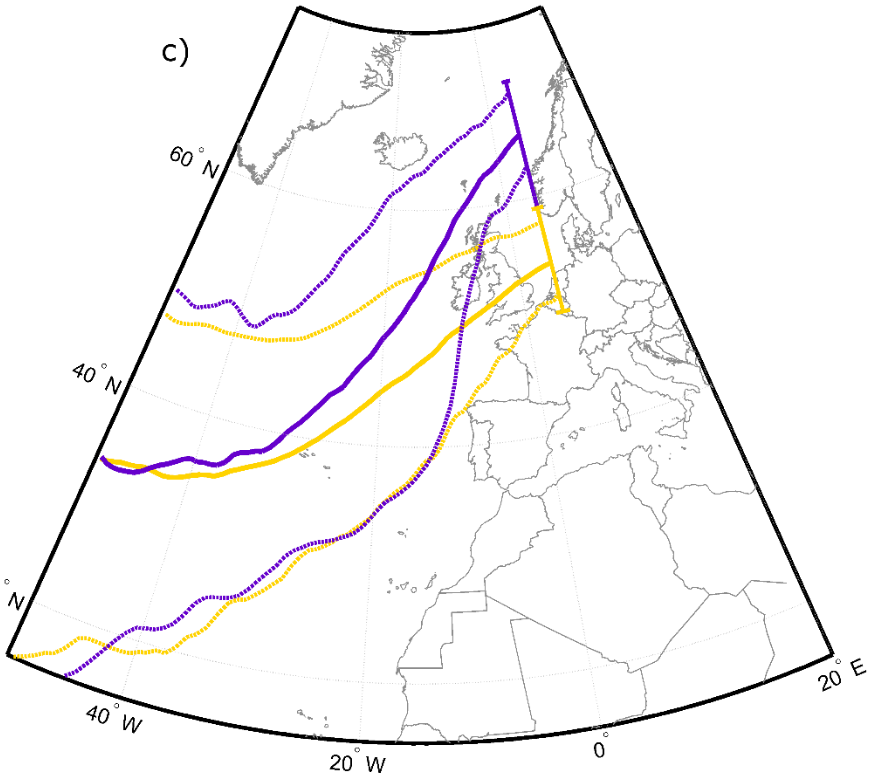

Figure 2.

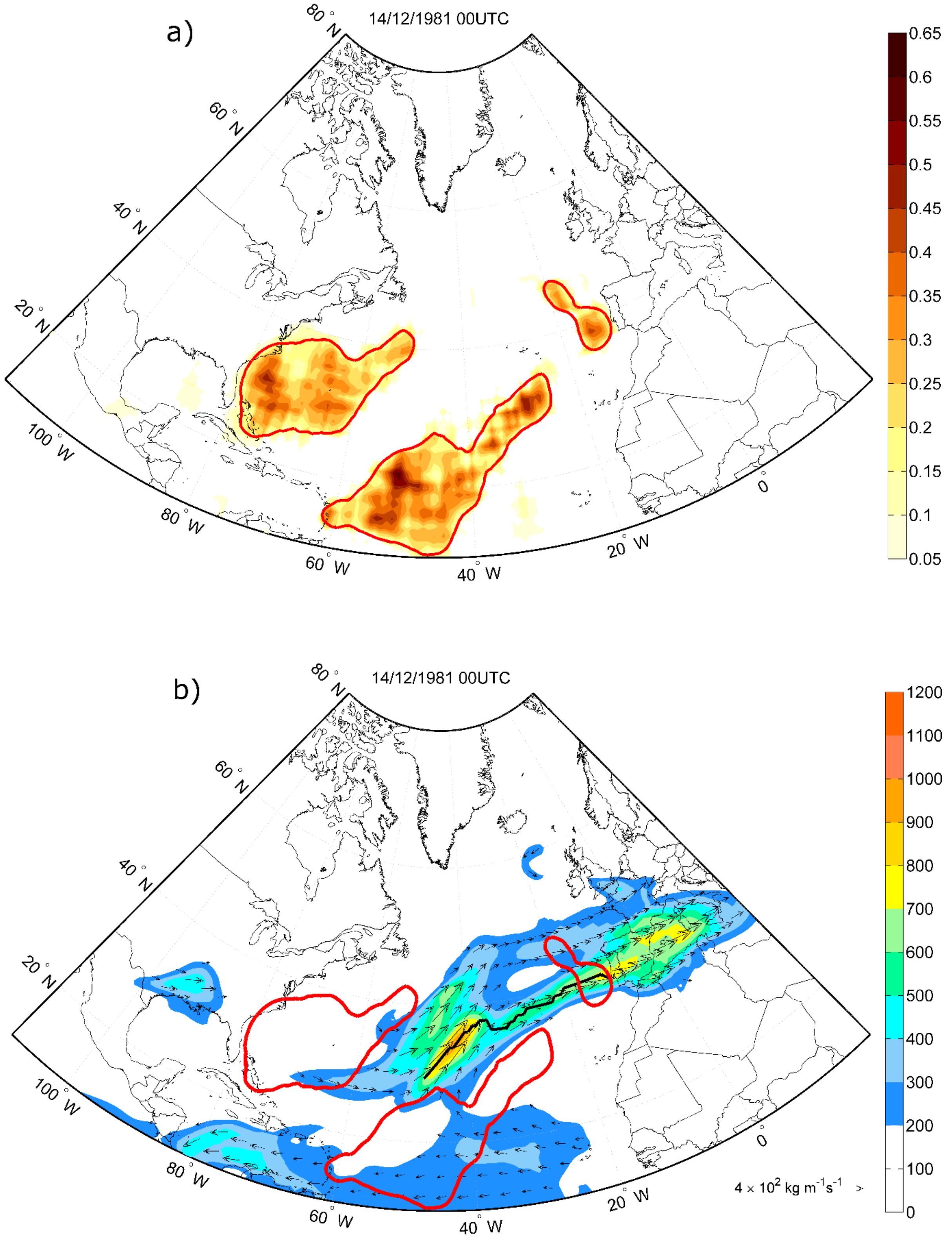
a)
14/12/1981 00UTC
80 °N
60 °N
40 °N
20 °N
100 °W
80 °W
60 °W
40 °W
20 °W
0
0.65
0.6
0.55
0.5
0.45
0.4
0.35
0.3
0.25
0.2
0.15
0.1
0.05
b)
14/12/1981 00UTC
80 °N
60 °N
40 °N
20 °N
100 °W
80 °W
60 °W
40 °W
20 °W
0
4 × 10^2 kg m^-1s^-1
1200
1100
1000
900
800
700
600
500
400
300
200
100
0

Figure 3.

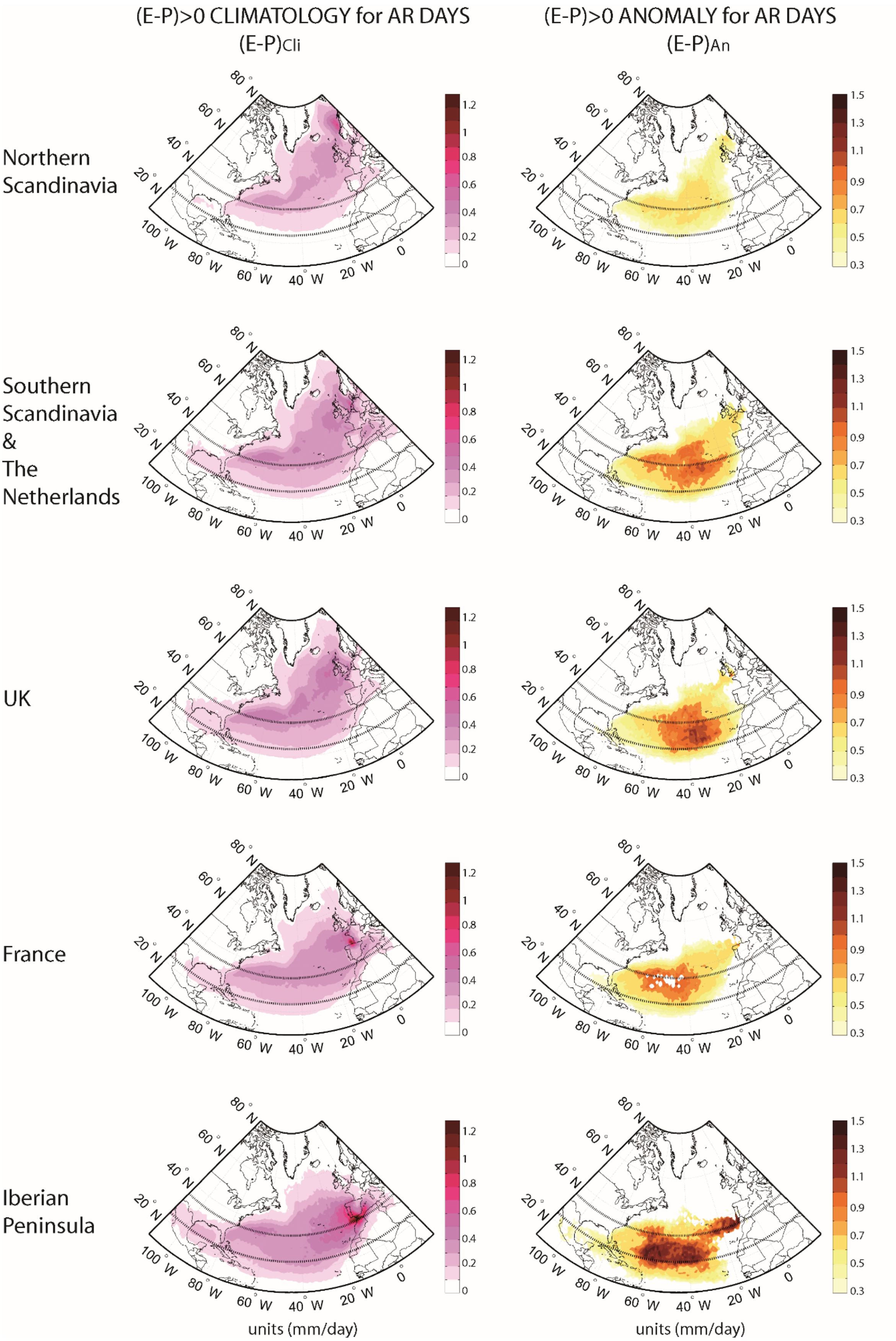

(E-P)>0 CLIMATOLOGY for AR DAYS
(E-P)Cli
(E-P)>0 ANOMALY for AR DAYS
(E-P)An
Northern Scandinavia
Southern Scandinavia & The Netherlands
UK
France
Iberian Peninsula
units (mm/day)
units (mm/day)

1

2 **Figure 4**

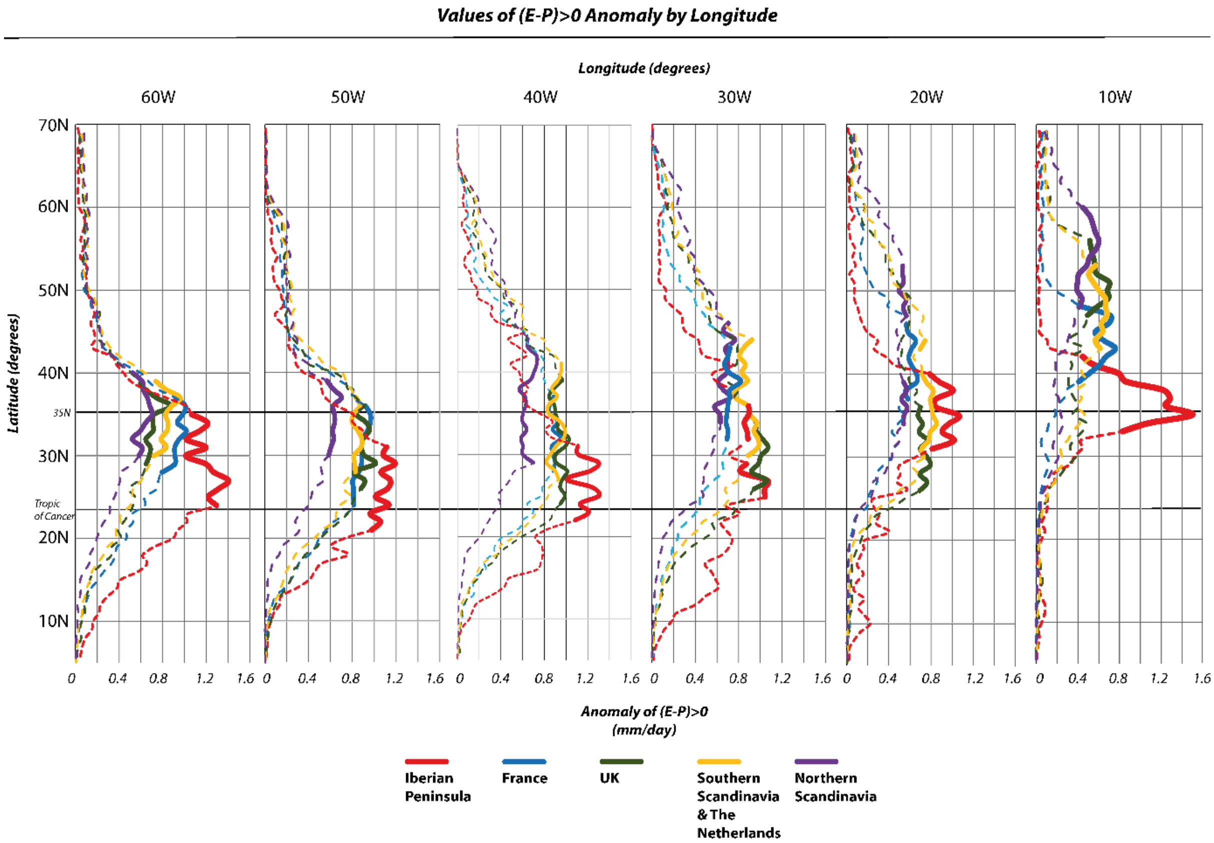
Values of (E-P)>0 Anomaly by Longitude
Longitude (degrees)
60W
50W
40W
30W
20W
10W
70N
60N
50N
40N
35N
30N
Tropic of Cancer
20N
10N
Latitude (degrees)
0
0.4
0.8
1.2
1.6
Anomaly of (E-P)>0 (mm/day)
Iberian Peninsula
France
UK
Southern Scandinavia & The Netherlands
Northern Scandinavia

1

2 **Figure 5.**